Pazopanib Enhances Paclitaxel-Induced Mitotic Catastrophe in Anaplastic Thyroid Cancer

Crescent R. Isham[1,2], **Ayoko R. Bossou**[1,2], **Vivian Negron**[3], **Kelly E. Fisher**[4], **Rakesh Kumar**[4], **Laura Marlow**[5], **Wilma L. Lingle**[3], **Robert C. Smallridge**[2,6], **Eric J. Sherman**[7], **Vera J. Suman**[2,8], **John A. Copland**[2,5], and **Keith C. Bible**[1,2,*]

[1]Division of Medical Oncology, Department of Oncology, Mayo Clinic, Rochester, MN 55905, USA.

[2]Endocrine Malignancies Disease Oriented Group, Mayo Clinic Cancer Center, Mayo Clinic, Rochester, MN 55905, USA.

[3]Division of Experimental Pathology, Department of Laboratory Medicine and Pathology, Mayo Clinic, Rochester, MN 55905,USA.

[4]Department of Cancer Biology and Research, GlaxoSmithKline, Collegeville, PA 19426, USA.

[5]Division of Experimental Pathology, Department of Biochemistry and Molecular Biology, Mayo Clinic, Jacksonville, FL 32224, USA.

[6]Division of Endocrinology, Mayo Clinic, Jacksonville, FL 32224, USA.

[7]Memorial Sloan-Kettering Cancer Center, New York, NY 10065, USA.

[8]Division of Biomedical Statistics and Informatics, Mayo Clinic, Rochester, MN 55905, USA.

Abstract

Anaplastic thyroid cancer (ATC) has perhaps the worst prognosis of any cancer, with a median survival of only about 5 months regardless of stage. Pazopanib monotherapy has promising clinical activity in differentiated thyroid cancers (generally attributed to vascular endothelial growth factor receptor inhibition), yet has less effective single-agent activity in ATC. We now report that combining pazopanib with microtubule inhibitors such as paclitaxel produced heightened and synergistic antitumor effects in ATC cells and xenografts that were associated with potentiated mitotic catastrophe. We hypothesized that combined effects may reflect enhanced paclitaxel-induced cytotoxicity mediated by cell cycle regulatory kinase inhibition by pazopanib. Indeed, pazopanib potently inhibited aurora A, with pazopanib/paclitaxel synergy recapitulated by aurora A short hairpin RNA knockdown or by specific aurora A pharmacological inhibition. Pazopanib/paclitaxel synergy was reversed by aurora A knockdown. Moreover, aurora A (but not B or C) message and protein levels were significantly increased in patient ATCs, and durable benefit resulted from pilot clinical translation of pazopanib/paclitaxel therapy in a patient with

*To whom correspondence should be addressed. Bible.keith@mayo.edu.

metastatic ATC. Collectively, these results suggest that the pazopanib/paclitaxel combination is a promising candidate therapeutic approach in ATC and that aurora A may represent a potentially viable therapeutic molecular target in ATC.

INTRODUCTION

Despite an overall decline in cancer mortality in the United States, thyroid cancer incidence has doubled in the past decade and increased by 75% in the past 5 years. Thyroid cancer is now the eighth most incident cancer overall, the fifth most incident cancer in women, and an emerging public health concern in the United States (1–5). With more than 56,000 new cases annually, thyroid cancer is now more frequently diagnosed in the United States than ovarian, pancreatic, or esophageal cancer or all leukemias combined (1, 5). Moreover, thyroid cancer is increasing worldwide and is now the second most incident cancer in women in the Middle East (6).

Although most thyroid cancer patients have excellent prognosis, thyroid cancer leads to >1700 deaths annually in the United States alone (1). For patients with aggressive disease, therapeutic options are very limited, with little benefit obtained from the use of cytotoxic chemotherapy in the most common histological variant, differentiated thyroid cancer (DTC) (7). The situation for patients afflicted with the most aggressive and deadly form of thyroid cancer, anaplastic thyroid cancer (ATC), is especially dire, because median survival regardless of stage is only about 5 months, with only 20% survival 1 year from diagnosis (8, 9). The last agent to be approved by the Food and Drug Administration for use in these cancers occurred in the 1970s. Improved therapies for both aggressive DTC and ATC are therefore sorely needed.

We recently reported that the kinase inhibitor pazopanib induced marked and durable clinical responses in about half of all DTC patients afflicted with otherwise radioactive iodine-refractory disease [49% RECIST (Response Evaluation Criteria in Solid Tumors) partial responses] (10). However, although several pazopanib-treated ATC patients in our recent phase 2 trial incurred transient disease regression, there were no RECIST responses (11). This stimulated interest in developing combinatorial strategies to better use pazopanib in treating ATC.

We now report results of investigations focused on identification of promising pazopanib-containing drug combinations, with primary emphasis on improving pazopanib therapeutic effects in ATC. These studies led us to identify the pazopanib/paclitaxel combination as promising and prompted us to investigate in detail the mechanism of aurora A as a potentially important candidate therapeutic molecular target in ATC. Our results have implications for future drug development beyond those just related to pazopanib because more selective aurora kinase inhibitors and/or inhibitors of other cell cycle–critical kinases appear also to represent additional promising candidate ATC therapeutics especially when combined with antimicrotubule agents.

RESULTS

Pazopanib monotherapy inhibits colony formation in ATC cells

Having observed encouraging clinical activity of pazopanib in DTC (10), we examined in parallel its preclinical effects in ATC. Pazopanib (Fig. 1A) inhibited colony formation both in commonly used validated ATC cell lines (Fig. 1B) and in low-passage patient primary ATC cells (Fig. 1C, validated to ensure concordance with the patient cancers from which they originated) (12) at concentrations [median inhibitory concentrations (IC_{50}s), 3 to 18

µM, Fig. 1D] easily attained in the plasma of DTC patients attaining clinical benefit treated in conjunction with our pazopanib monotherapy clinical trial (10). Strikingly, pazopanib inhibited colony formation in ATC lines with similar IC_{50}s to those attained in DTC lines (Fig. 1D), prompting further studies of the effects of pazopanib in ATC. These results also indicated that, in addition to potentially affecting vascular endothelial growth factor (VEGF) signal transduction in tumor vasculature in vivo, pazopanib also has direct antiproliferative effects on both ATC and DTC cells even in the absence of the tumor microenvironment.

Pazopanib potentiates the antineoplastic effects of paclitaxel and other antimicrotubule inhibitors in ATC in vitro and in vivo

When screening an array of therapeutics in a panel of thyroid cancer cell lines, we consistently observed synergy when pazopanib and paclitaxel were combined. Paclitaxel is also of particular interest in ATC because of a previous study indicating single-agent clinical efficacy in ATC (13). We used two independent experimental approaches to examine potential synergy between pazopanib and paclitaxel. First, pazopanib consistently potentiated paclitaxel-induced attenuation of colony formation in all tested ATC cell line models (Fig. 2, A, E, and F; $P < 0.01$) at concentrations that had no or modest single-agent effects (2.5 µM; see Fig. 1B); similar potentiation was also observed in low-passage primary patient THJ11T ATC cells (Fig. 2C; $P < 0.01$). In parallel experiments assessing synergy in an entirely different fashion per the median-effect analysis approach of Chou and Talalay (14), formal statistical analyses also confirmed pazopanib/paclitaxel synergy in ATC, with combination indices (CIs) consistently well below 1.0 (indicating synergy) both in ATC cell lines (for example, KTC2; Fig. 2B) and in primary ATC cells (for example, THJ11T; Fig. 2D). Moreover, pazopanib synergistically combined with all tested additional antimicrotubule inhibitors including the Vinca alkaloid vincristine (Fig. 2G), the taxane docetaxel (Fig. 2H), as well as the epothilone ixabepilone (Fig. 2I), suggesting a class effect across microtubule inhibitors of varying chemical structures.

Enhanced effects were also demonstrated in vivo, whereby combined pazopanib/paclitaxel reduced tumor volumes by >50% relative to paclitaxel or pazopanib monotherapy at later time points in KTC2 ATC xenografts (Fig. 3A), bolstering support for the possibility that the pazopanib/paclitaxel combination might also have promise when translated to patients afflicted with ATC. Indeed, a single (pilot) ATC patient with lung metastases treated with pazopanib (400 to 800 mg/day, orally) and paclitaxel (50 to 80 mg/m^2 per week, intravenously) attained marked and durable regression of metastatic disease (confirmed RECIST response; Fig. 3B). Although this result is anecdotal, it demonstrates feasibility of clinical translation of the combination; moreover, the occurrence of durable benefit in metastatic ATC in response to any therapy is remarkable (8).

Subsequent experiments were conducted to attempt to uncover mechanisms underlying the observed pazopanib/paclitaxel synergy. On the basis of our previous experience indicating that the adenosine triphosphate (ATP)–mimetic small-molecule cyclin-dependent kinase (CDK) inhibitor flavopiridol greatly enhances the cytotoxic effects of paclitaxel (15), we hypothesized that a mechanism underlying the observed pazopanib/paclitaxel synergy might similarly reflect inhibition of cell cycle regulatory kinases by pazopanib, thereby resulting in altered cell cycle exit and consequently increased levels of commitment to cell death (mitotic catastrophe).

Pazopanib potentiates the cell cycle effects of paclitaxel

In examining the possibility that pazopanib might act in part by potentiating the cell cycle effects of paclitaxel, we first undertook fluorescence-activated cell sorting (FACS) analyses. Whereas pazopanib alone led to dose-dependent decreases in the fraction of cells in S and

G_2-M phases of the cell cycle (Fig. 4, A to D; $P < 0.01$, Fig. 4, K and L) and paclitaxel alone led to slight increases in S and G_2-Mphase cells (Fig. 4, E to G; NS, Fig. 4, K and L), the addition of pazopanib to paclitaxel heightened the proportion of KTC2 cells in S phase and especially that of G_2-M cells in response to paclitaxel monotherapy ($P < 0.05$; Fig. 4, K and L). In particular, the addition of 5 μM pazopanib to 10 nM paclitaxel led to a ~50% increase in the proportion of cells in the G_2-M phase of the cell cycle in comparison to that attained from 10 nM paclitaxel monotherapy, suggesting that pazopanib/paclitaxel synergy might be in part attributable to the combined cell cycle effects of pazopanib and paclitaxel, prompting additional more refined studies.

Time-lapse video microscopy was next used to more specifically interrogate combined effects via continuously monitoring individual KTC2 ATC cells over 48-hour periods of exposure to pazopanib, paclitaxel, or the combination (Fig. 5A, screen capture images at the beginning and end of treatments, to illustrate net effects of various treatments on proliferation; Fig. 5B, tabulated data indicating fates of cells followed continuously over 48-hour treatment periods). Although 2.5 μM pazopanib monotherapy neither affected the fractions of morphologically normal, multinucleated, or dead cells subject to death attributable to dysfunctional cell division ("mitotic catastrophe"; see Fig. 5B, all panels, NS) nor altered the frequency of paclitaxel-induced multinucleation (Fig. 5B, middle panel, NS), remarkably, the same pazopanib concentration, when added to paclitaxel, doubled cell death associated with mitotic catastrophe in comparison to paclitaxel monotherapy (Fig. 5B, right panel; $P < 0.05$), thereby providing a potential phenomenological explanation for the observed cytotoxic synergy.

Pazopanib inhibits the activity of aurora kinases in cell-free assays and in intact ATC cells, and aurora A, but not aurora B or C, is overexpressed in ATC

Collectively, FACS and video microscopy results led us to postulate that the cell cycle effects of pazopanib might be responsible for its observed ability to synergize with and augment paclitaxel-induced mitotic catastrophe. Because we had previously observed marked cytotoxic synergy when combining the CDK inhibitor flavopiridol with paclitaxel (14), we were leaning toward the possibility that inhibition of the function of cell cycle–critical kinases such as cyclin-dependent, Pololike, and/or aurora kinases by an ATP-mimetic kinase inhibitor like pazopanib might account for the observed pazopanib/paclitaxel synergy. Indeed, aurora kinase inhibition has also been reported by others to synergize with paclitaxel (16, 17). We therefore investigated whether pazopanib might inhibit an array of cell cycle regulatory kinases with potential to contribute to observed synergy. Although the cell-free IC_{50} for the inhibition of cyclin-dependent kinases (CDKs) 1 and 2 and also for Polo-like kinase 1 (PLK-1) were >1000-fold higher than that of VEGF receptors (VEGF-Rs) (18), we found that the IC_{50} values with respect to the inhibition of aurora kinases A and B by pazopanib were 167 ± 15.5 nM and 254 ± 29.8 nM, respectively (mean ± SD, Fig. 6A)—within 10-fold of analogous IC_{50}s (10 to 50 nM) with respect to VEGF-R_{1-3}, concentrations achieved both experimentally and clinically (10). These data led us to conduct further studies of the roles of aurora kinases in ATC.

We reasoned that aurora A might be overexpressed in ATC as a potential explanation for observed impressive single-agent and combined effects of pazopanib in ATC models, wondering whether aurora kinases might specifically represent potentially important ATC therapeutic molecular targets. We focused on ATC in this context in part because paclitaxel monotherapy has proven clinical efficacy in ATC (13), yet not in DTC (7), reasoning that clinical translation of the pazopanib/paclitaxel combination might therefore be expected to have greatest potential in ATC (as illustrated in the case of an ATC patient treated with the combination as depicted in Fig. 3B). Furthermore, given the demonstrated strong clinical

activity of pazopanib monotherapy in DTC, it was unclear whether the pazopanib/paclitaxel combination would have sufficiently greater incremental activity to merit translation into DTC.

In examining aurora A mRNA levels using transcriptional profiling in 12 nonneoplastic patient thyroid tissue samples versus 13 ATC patient tumors, we found that aurora A message was 5.0-fold higher in ATC samples (1433 ± 830 versus 286 ± 154, mean $\pm$ SD, $P < 0.05$), indicating that aurora A message is relatively overexpressed in ATC. In comparison, neither aurora B nor aurora C messages were significantly altered. Hence, although pazopanib inhibited both aurora A and B (Fig. 6A), ATC expression data pointed to aurora A as of greater potential clinical relevance in ATC.

We next examined aurora kinase protein levels in patient samples using immunohistochemistry (Fig. 6B shows representative staining results; Fig. 6C shows tabulated data). Whereas aurora B protein expression did not differ significantly between normal thyroid and ATC, the proportion of those with aurora A protein expression was significantly higher in ATC ($12.78 \pm 13.78\%$ versus $1.29 \pm 1.55\%$ grade 3 staining, mean $\pm$ SD, $P < 0.05$; Fig. 6C); aurora C was undetectable via immunohistochemistry. On the basis of these results and the rationale articulated above, our further studies focused primarily on aurora A because it appeared to be more relevant to ATC pathogenesis in comparison to other aurora kinases and, consequently, a potentially more viable candidate ATC therapeutic molecular target.

We therefore next examined whether pazopanib might inhibit aurora A autophosphorylation in intact ATC cells. Consistent with inhibition of aurora A activity not only in cell-free conditions (Fig. 6A) but also in intact ATC cells, decreases in levels of phospho–aurora A were observed in response to exposure of mitotic/synchronized KTC2 or THJ11T ATC cells to pazopanib; these effects were of similar magnitudes to those observed in response to parallel (positive control) treatment with the specific pharmacological aurora A inhibitor MLN8237 and were observed at pazopanib concentrations producing synergistic effects with paclitaxel (Fig. 6D, multiple replicate KTC2 experimental results summarized in Fig. 6E). Although we also undertook detailed multi–time point immunofluorescence studies examining the cellular localization of centrin, aurora A, and phospho–aurora A in intact cells treated with pazopanib, paclitaxel, and the combination (analogous to the light microscopy studies depicted in Fig. 5), these additional studies failed to add further mechanistic clarity, leading us to specifically examine the potential roles of aurora kinases in ATC using other approaches. In particular, to further evaluate the possibility that aurora A inhibition by pazopanib might be of therapeutic relevance, we next specifically examined (i) the effects of aurora A knockdown or pharmacological aurora A inhibition in ATC, and (ii) whether the effects of pazopanib on aurora A might specifically contribute to pazopanib/paclitaxel synergy in ATC.

Inhibition of aurora A by pazopanib appears to contribute to pazopanib/paclitaxel synergy

To examine whether inhibition of the cell cycle–critical kinase aurora A by pazopanib might specifically contribute to pazopanib/paclitaxel synergy, we assessed the effects of short hairpin RNA (shRNA) aurora A knockdown in KTC2 ATC cells, hypothesizing that shRNA aurora A knockdown alone might prove synergistic with paclitaxel. We further hypothesized that aurora A knockdown might blunt paclitaxel/pazopanib synergy, provided that the underlying mechanism of pazopanib/paclitaxel synergy depends on aurora A inhibition by pazopanib; we reasoned that maximal aurora A shRNA knockdown would render further attenuation of aurora A activity by pazopanib impossible. However, complete knockdown of aurora A results in cytotoxicity (aurora A is critical to cell cycle traverse). We consequently sought to achieve only partial shRNA aurora A down-regulation. When achieved (see

immunoblotting results for clones sh2 to sh4; Fig. 7A, inset), increased sensitivity to paclitaxel in shRNA aurora A knockdown clones relative to nontarget control clones was observed (Fig. 7A), consistent with our hypothesis that aurora A inhibition heightens paclitaxel sensitivity in ATC. Moreover, pazopanib/paclitaxel synergy was also consistently attenuated in shRNA aurora A knockdown clones (Fig. 7B), confirming involvement of aurora A inhibition by pazopanib in the observed pazopanib/paclitaxel synergy.

To assess in parallel whether more selective pharmacological inhibition of aurora A might also synergize with paclitaxel to produce heightened antineoplastic effects, we next examined the effects of inhibition of aurora A using MLN8237. Indeed, marked synergy was observed when combining MLN8237 and paclitaxel (KTC2 ATC cells, median-effect analysis CI plot shown in Fig. 7C), again consistent with the hypothesis that aurora A inhibition potentiates paclitaxel-induced anticancer effects in ATC, mirroring the findings of shRNA aurora A knockdown experiments (Fig. 7A), and when combining paclitaxel and pazopanib (Fig. 2). Comparison of the effects of pazopanib (2.5 μM) and the aurora A inhibitor MLN8237 (25 nM) on the inhibition of KTC2 ATC colony formation by paclitaxel is shown in Fig. 6D, indicating that both agents similarly boost the anticancer effects of paclitaxel. Hence, obtained results indicate that either pharmacologic or molecular aurora A inhibition/knockdown potentiates the antineoplastic effects of paclitaxel in ATC and, moreover, that the observed pazopanib/paclitaxel synergy appears to arise at least in part from the unexpected inhibition of aurora A by pazopanib.

DISCUSSION

Here, we attempt to better define opportunities for optimizing pazopanib as a candidate therapeutic in ATC. We had previously found pazopanib monotherapy to have disappointing clinical activity in ATC (11); therefore, we investigated combinatorial therapeutic approaches that led to the discovery of enhanced antineoplastic effects when combining pazopanib and antimicrotubule inhibitors in ATC model systems. Enhanced combined effects were attributable to inhibition of aurora A by pazopanib, and inhibitors of aurora kinases (and perhaps inhibitors of cell cycle–critical kinases in general) may represent attractive candidate therapeutics in ATC, especially when combined with microtubule inhibition.

Pazopanib/paclitaxel synergy was observed not only in vitro but also in vivo: Pilot anecdotal data from an ATC patient treated with the combination suggested marked and durable regression of metastatic disease. On this basis, a Radiation Therapy Oncology Group (RTOG) randomized clinical trial has been developed and activated, comparing paclitaxel monotherapy to the pazopanib/paclitaxel doublet when administered in parallel with intensity-modulated neck radiation therapy in ATC (ClinicalTrials.gov identifier NCT01236547).

From the mechanistic standpoint, the observed synergy was found to be associated with heightened paclitaxel-induced mitotic catastrophe, with the underlying mechanism defined here being relate to the inhibition of aurora A kinase by pazopanib. These data indicate that previously unanticipated "off-target" effects of pazopanib on aurora A may affect its clinical application and use, especially when combined with antimicrotubule inhibitors.

Our investigations into the mechanisms underlying the synergy between pazopanib and antimicrotubule agents in ATC have heightened our awareness of the potential significance of aurora kinases as candidate therapeutic molecular targets in thyroid cancers, especially in ATC, where we found a high degree of aurora A overexpressed at the mRNA level (and correspondingly increased at the protein level). The plausibility of aurora A as a candidate

ATC therapeutic molecular target is further supported by data indicating that the augmentation of antimicrotubule agent–induced cytotoxicity by pazopanib can be recapitulated either by shRNA knockdown of aurora A or by the specific aurora A inhibitor MLN8237. Consequently, opportunities for combining antimicrotubule inhibitors with aurora A inhibitors more specific than pazopanib also appear to hold translational promise in ATC. Indeed, other groups have previously reported single-agent effects of pharmacological inhibition of aurora kinases in ATC (19, 20). Pazopanib/paclitaxel synergy has also been described in nonthyroid cancer models (17, 21–23), albeit apparently not previously in ATC, indicating that the finding may be generalizable across multiple tumor types and have application beyond ATC.

The relative extents to which aurora A and B may be important in cancer pathogenesis in general—or in thyroid cancer pathogenesis in particular—remain in dispute in the literature. Although our data indicate a role of aurora A in ATC, other studies point instead to a potential role of aurora B. In particular, Sorrentino *et al.* reported aurora B overexpression in ATC relative to DTC and additionally found in vivo antitumor effects resulting from antisense aurora B treatment (24). However, the ARO cell line used in some experiments was recently found not to represent thyroid cancer (25) and the comparison group was DTC and not normal thyroid tissue, thereby drawing into question the voracity of reported results. Much akin to our present report, however, Wiseman *et al.* instead found that aurora A was overexpressed in 41% of examined ATC patient samples, but that aurora B was not (26). Hence, although aurora A collectively seems of greater importance in ATC pathogenesis, the precise relative contributions to which aurora A and B may be important in thyroid and other cancers of differing histotypes remain to be better defined.

It is also unclear why pazopanib monotherapy might lead to a decrease in the fraction of ATC cells in the G_2-M phase of the cell cycle, as opposed to the expected increase in G_2-M fraction in response to therapy with a specific inhibitor of aurora A (20). We hypothesize that the decreased G_2-M fraction consequent to pazopanib treatment likely reflects the combined effects of pazopanib on multiple competing targets affecting cell cycle progression.

Recently, Gizatullin *et al.* reported that cancers lacking intact DNA damage response checkpoints attributable to dysfunctional p53 pathways are more susceptible to apoptosis induction when treated with the aurora kinase inhibitor VX-680 (27), raising the question of whether ATC, which frequently has mutated p53, may be especially sensitive to aurora kinase inhibitors. In our experiments, however, pazopanib produced overall qualitatively similar in vitro results in p53 wild-type (KTC2) and mutant (KTC3) cell lines, leaving this important question in need of further investigation.

In summary, our studies indicate that pazopanib and antimicrotubule inhibitors including paclitaxel combine synergistically in ATC models observed in association with heightened induction of mitotic catastrophe apparently attributable to the inhibition of aurora A by pazopanib. Further, aurora A (but not aurora B or C) is up-regulated in ATC, and specific aurora A inhibitors (such as MLN8237) or aurora A knockdown similarly combines synergistically with antimicrotubule inhibition in ATC. Moreover, we have also shown that pazopanib/paclitaxel synergy is observed not only in vitro but also in vivo, with pilot translation of these data producing encouraging preliminary results in human ATC. Collectively, we believe that the presented data provide compelling rationale not only for further evaluation of the paclitaxel/pazopanib combination in ATC but also for further study of the specific roles and therapeutic relevance of inhibition of aurora and other cell cycle–critical kinases in ATC, especially when combined with inhibition of microtubule function.

MATERIALS AND METHODS

Tissue culture

Thyroid cell lines (from J.A.C., validated by genotyping) were cultured in RPMI 1640 with L-glutamine containing nonessential amino acids, sodium pyruvate, Hepes, sodium bicarbonate, penicillin G (100 U/ml), and streptomycin (100 μg/ml) also containing 10% fetal bovine serum and were passaged twice weekly.

Colony formation assays

Briefly, 400 subconfluent cells were plated on triplicate sets of 35-mm dishes, allowed to adhere overnight, and then treated with diluent or drugs as specified. In synergy experiments, pazopanib was added 1 to 2 hours before other drugs (paclitaxel, vincristine, docetaxel, and ixabepilone); plates were washed after 24-hour drug exposures, with pazopanib added back after washing. After 6 to 10 days, plates were stained with Coomassie blue, with colonies counted on an imager using GeneTools software (Syngene). CalcuSyn software (BioSoft) was used to assess synergy; data were plotted as dose-effect curves with the Chou and Talalay median-effect method (14).

Flow cytometry (FACS)

KTC2 cells treated as indicated were harvested, washed twice in cold phosphate-buffered saline (PBS), fixed by dropwise addition of cold 95% ethanol, incubated at 0°C for >1 hour, rehydrated and washed twice with PBS, and incubated with ribonuclease A (1 mg/ml) (15 min, 37°C) and subsequently with propidium iodide (100 μg/ml) (Sigma), both in 0.1% aqueous sodium citrate. Samples were evaluated on a FACSCalibur (Becton Dickinson; 488-nm excitation, 585/42-nm filter) by the Mayo Flow Cytometry Core Facility. Data for cell cycle were analyzed with ModFit LT software (Verity Software House), with subdiploid debris specifically excluded from analysis (to assess cell cycle distribution of live/surviving cells).

Cell video microscopy

Low-confluence KTC2 cells in 12-well plates treated with pazopanib 1 hour before paclitaxel addition were video-imaged (every 15 min for 48 hours) while incubated in a temperature- and humidity-controlled environment, with the data collected by an ApoTome microscope (Carl Zeiss, 10× objective in bright field) using AxioVision LE software (Carl Zeiss). Cell fates (continuously observed) at 48 hours were critically analyzed visually/morphologically and plotted as percent time = 0 cells (cells not continuously visualized were excluded from analyses). Only cells that were observed to undergo mitosis followed by apoptotic disintegration were tabulated as cells dead from mitotic events.

Aurora kinase assays

Aurora A(2–403) and aurora B(2–344) full-length constructs were expressed and purified in-house at GlaxoSmithKline (by K.E.F. and R.K.). TPX2(1–43) peptide was synthesized by California Peptide Research Inc., whereas INCENP(826–919) was expressed and purified by the University of Dundee (Scotland). Peptide substrates [5FAM-GRTGRRNSI-NH2 for IMAP (immobilized metal ion affinity-based fluorescence polarization) assays] were custom-synthesized by 21st Century Biochemicals. IMAP Progressive Binding Reagent (nanoparticles/beads) and Buffers were obtained from Molecular Devices Inc. All other reagents were obtained from Sigma. IMAP assays were used to assess aurora A or B kinase inhibition and were conducted according to previously reported methods (16), with results expressed as percentages of control (uninhibited) values.

Lentiviral shRNA aurora A knockdown

A Sigma MISSION shRNA vector clone set against Aurora A (Sigma) was obtained via Mayo RISR (RNA Interference Shared Resource, Mayo Clinic). Vector DNA was amplified from bacterial stocks and purified with Qiagen EndoFree Maxiprep kit. Viral particles were produced in human embryonic kidney (HEK) 293T by transfection of each clone along with packaging vectors vsvg and gag pol (received as a gift from V. Shridhar's laboratory, Mayo Clinic) with ExpressFect Transfection Reagent (Denville Scientific). Viral supernatant was collected at 48 hours and used for transduction of KTC2 cells. A double transduction was done with 3 ml of viral supernatant per 100-mm dish, with polybrene (8 μg/ml) (Sigma) added on 2 consecutive days. Selection with puromycin (1 μg/ml) was performed for 10 to 12 days before Western blot and colony-forming assays. Viable stable lines with best knockdown were achieved from clone 3 (NM_003600.x-985s1c1) and clone 4 (NM_003600.x-1252s1c1) with the following target sequences: CCTGTCTTACTGTCATTCGAA and CACATACCAAGAGACCTACAA.

Immunoblotting

KTC2 cells in log-phase growth were synchronized [nocodazole (0.5 μg/ml) overnight], shaken to release mitotic cells that were washed twice with media, plated, and then treated for 30 min with diluent, pazopanib, or MLN8237 as indicated. Thereafter, cells were lysed [10 mM tris (pH 7.4) + 1% SDS with protease inhibitor cocktail (Roche) and 1 mM sodium orthovanadate (Sigma)], sonicated, loaded on triplicate gels for SDS–polyacrylamide gel electrophoresis (based on equal protein), transferred onto nitrocellulose membranes, and blotted for phospho–aurora A (Cell Signaling Technology), aurora A (AbD Serotec), centrin (a gift from J. Salisbury's laboratory, Mayo Clinic), and actin (Santa Cruz Biotechnology).

Immunohistochemistry

Use of deidentified human tissues was approved by the Mayo Institutional Review Board. Thyroid tissues mounted on slides from paraffin-embedded blocks and blocked with diluent containing Background Reducing Components (Dakocytomation, 30 min) were probed for aurora A (AbD Serotec) or aurora B (Santa Cruz Biotechnology). Negative control sections were prepared by incubation in the absence of primary antibody. Images were obtained at 20× (ScanScope XT and ImageScope software; Aperio Technologies) with staining scored using an algorithm based on signal intensity (0 to 3+).

Assessment of aurora kinase mRNA levels

Aurora kinase A, B, and C mRNA levels in patient ATC tissues were assessed in replicate with transcriptional profiling (Affymetrix U133 2.0 platform).

Xenograft studies

All mouse experiments followed institutional guidelines and were approved by the Mayo Clinic Institutional Animal Care and Use Committee (IACUC). Briefly, KTC2 cells washed twice and resuspended in PBS/Matrigel (1:1; 7.5 million cells/100 μl) were injected subcutaneously (100 μl of KTC2 inoculum per animal) in the flanks of female athymic nu/nu mice (6 weeks old; Harlan Laboratories Inc.) anesthetized with isoflurane. After 4- to 5-mm tumors formed, mice randomly assigned to groups (of 10 animals each) were fed OpenStandard diet (Research Diets Inc.) with or without pazopanib (287.5 mg/kg). Paclitaxel reconstituted in saline was administered intraperitoneally. Tumors were measured twice weekly, with tumor volumes calculated as follows: $A \times B \times B/2$, where A is the longest dimension and B, the smallest. In parallel, animal weights were monitored to ensure tolerance of administered therapies. Animals showing distress of tumor ulceration were euthanized according to the IACUC guidelines.

Patient data

Examination of the combined effects of pazopanib (800 mg/day, orally) and paclitaxel (80 mg/m^2 per week, intravenously) therapy in a pilot ATC patient was approved by the involved local Institutional Review Board, with written informed consent in parallel provided by the patient. Because this patient was subjected, in parallel, to neck radiotherapy, for the purposes of this article, only the effects on metastatic tumor deposits in the lung were shown to ensure that displayed results were indicative of those resulting from systemic therapy alone.

Statistical analyses

Two-sided *t* tests were used to assess differences in mean (i) percentages of colonies formed in vitro, (ii) tumor volumes in vivo, or (iii) percentages of cells with 3+ staining of aurora A or aurora B. One-sided *t* tests were used to examine differences in fractions of morphologically normal, multinucleated, or dead cells in video microscopy experiments or in fractions of cells in S and G_2-M phases of the cell cycle.

Acknowledgments

REFERENCES AND NOTES

1. Cancer Facts & Figures 2010. Atlanta, GA: American Cancer Society; 2010. American Cancer Society.

2. Chen AY, Jemal A, Ward EM. Increasing incidence of differentiated thyroid cancer in the United States, 1988–2005. Cancer. 2009; 115:3801–3807. [PubMed: 19598221]

3. Enewold L, Zhu K, Ron E, Marrogi AJ, Stojadinovic A, Peoples GE, Devesa SS. Rising thyroid cancer incidence in the United States by demographic and tumor characteristics, 1980–2005. Cancer Epidemiol. Biomarkers Prev. 2009; 18:784–791. [PubMed: 19240234]

4. Hayat MJ, Howlader N, Reichman ME, Edwards BK. Cancer statistics, trends, and multiple primary cancer analyses from the Surveillance, Epidemiology, and End Results (SEER) Program. Oncologist. 2007; 12:20–37. [PubMed: 17227898]

5. Jemal A, Siegel R, Ward E, Hao Y, Xu J, Thun MJ. Cancer statistics, 2009. CA Cancer J. Clin. 2009; 59:225–249. [PubMed: 19474385]

6. Al-Eid, HS.; Arteh, SO. Cancer Incidence Report Saudi Arabia 2003. Kingdom of Saudi Arabia: Ministry of Health National Cancer Registry; 2003.

7. Baudin E, Schlumberger M. New therapeutic approaches for metastatic thyroid carcinoma. Lancet Oncol. 2007; 8:148–156. [PubMed: 17267329]

8. Smallridge RC, Copland JA. Anaplastic thyroid carcinoma: Pathogenesis and emerging therapies. Clin. Oncol. (R. Coll. Radiol.). 2010; 22:486–497. [PubMed: 20418080]

9. McIver B, Hay ID, Giuffrida DF, Dvorak CE, Grant CS, Thompson GB, van Heerden JA, Goellner JR. Anaplastic thyroid carcinoma: A 50-year experience at a single institution. Surgery. 2001; 130:1028–1034. [PubMed: 11742333]

10. Bible KC, Suman VJ, Molina JR, Smallridge RC, Maples WJ, Menefee ME, Rubin J, Sideras K, Morris JC III, McIver B, Burton JK, Webster KP, Bieber C, Traynor AM, Flynn PJ, Goh BC, Tang H, Ivy SP, Erlichman C. Endocrine Malignancies Disease Oriented Group; Mayo Clinic Cancer Center; Mayo Phase 2 Consortium, Efficacy of pazopanib in progressive, radioiodine-

refractory, metastatic differentiated thyroid cancers: Results of a phase 2 consortium study. Lancet Oncol. 2010; 11:962–972. [PubMed: 20851682]

11. Bible KC, Suman VJ, Menefee ME, Smallridge RC, Molina JR, Maples WJ, Karlin NJ, Traynor AM, Kumar P, Goh BC, Lim WT, Bossou AR, Isham CR, Webster KP, Kukla AK, Bieber C, Burton JK, Harris P, Erlichman C. Mayo Phase 2 Consortium; Mayo Clinic Endocrine Malignances Disease Oriented Group, A multiinstitutional phase 2 trial of pazopanib monotherapy in advanced anaplastic thyroid cancer. J. Clin. Endocrinol. Metab. 2012; 97:3179–3184. [PubMed: 22774206]

12. Marlow LA, D'Innocenzi J, Zhang Y, Rohl SD, Cooper SJ, Sebo T, Grant C, McIver B, Kasperbauer JL, Wadsworth JT, Casler JD, Kennedy PW, Highsmith WE, Clark O, Milosevic D, Netzel B, Cradic K, Arora S, Beaudry C, Grebe SK, Silverberg ML, Azorsa DO, Smallridge RC, Copland JA. Detailed molecular fingerprinting of four new anaplastic thyroid carcinoma cell lines and their use for verification of RhoB as a molecular therapeutic target. J. Clin. Endocrinol. Metab. 2010; 95:5338–5347. [PubMed: 20810568]

13. Ain KB, Egorin MJ, DeSimone PA. Treatment of anaplastic thyroid carcinoma with paclitaxel: Phase 2 trial using ninety-six-hour infusion. Collaborative Anaplastic Thyroid Cancer Health Intervention Trials (CATCHIT) Group. Thyroid. 2000; 10:587–594. [PubMed: 10958311]

14. Chou TC, Talalay P. Analysis of combined drug effects: A new look at a very old problem. Trends Pharmacol. Sci. 1983; 4:450–454.

15. Bible KC, Kaufmann SH. Cytotoxic synergy between flavopiridol (NSC 649890, L86-8275) and various antineoplastic agents: The importance of sequence of administration. Cancer Res. 1997; 57:3375–3380. [PubMed: 9269999]

16. Curry J, Angove H, Fazal L, Lyons J, Reule M, Thompson N, Wallis N. Aurora B kinase inhibition in mitosis: Strategies for optimising the use of aurora kinase inhibitors such as AT9283. Cell Cycle. 2009; 8:1921–1929. [PubMed: 19440047]

17. Mazumdar A, Henderson YC, El-Naggar AK, Sen S, Clayman GL. Aurora kinase A inhibition and paclitaxel as targeted combination therapy for head and neck squamous cell carcinoma. Head Neck. 2009; 31:625–634. [PubMed: 19107951]

18. Kumar R, Knick VB, Rudolph SK, Johnson JH, Crosby RM, Crouthamel MC, Hopper TM, Miller CG, Harrington LE, Onori JA, Mullin RJ, Gilmer TM, Truesdale AT, Epperly AH, Boloor A, Stafford JA, Luttrell DK, Cheung M. Pharmacokinetic-pharmacodynamic correlation from mouse to human with pazopanib, a multikinase angiogenesis inhibitor with potent antitumor and antiangiogenic activity. Mol. Cancer Ther. 2007; 6:2012–2021. [PubMed: 17620431]

19. Wunderlich A, Fischer M, Schlosshauer T, Ramaswamy A, Greene BH, Brendel C, Doll D, Bartsch D, Hoffmann S. Evaluation of Aurora kinase inhibition as a new therapeutic strategy in anaplastic and poorly differentiated follicular thyroid cancer. Cancer Sci. 2011; 102:762–768. [PubMed: 21214672]

20. Arlot-Bonnemains Y, Baldini E, Martin B, Delcros JG, Toller M, Curcio F, Ambesi-Impiombato FS, D'Armiento M, Ulisse S. Effects of the Aurora kinase inhibitor VX-680 on anaplastic thyroid cancer-derived cell lines. Endocr. Relat. Cancer. 2008; 15:559–568. [PubMed: 18430894]

21. Lentini L, Amato A, Schillaci T, Insalaco L, Di Leonardo A. Aurora-A transcriptional silencing and vincristine treatment show a synergistic effect in human tumor cells. Oncol. Res. 2008; 17:115–125. [PubMed: 18669163]

22. Scharer CD, Laycock N, Osunkoya AO, Logani S, McDonald JF, Benigno BB, Moreno CS. Aurora kinase inhibitors synergize with paclitaxel to induce apoptosis in ovarian cancer cells. J. Transl. Med. 2008; 6:79. [PubMed: 19077237]

23. Mazumdar A, Henderson YC, El-Naggar AK, Sen S, Clayman GL. Aurora kinase A inhibition and paclitaxel as targeted combination therapy for head and neck squamous cell carcinoma. Head Neck. 2009; 31:625–634. [PubMed: 19107951]

24. Sorrentino R, Libertini S, Pallante PL, Troncone G, Palombini L, Bavetsias V, Spalletti-Cernia D, Laccetti P, Linardopoulos S, Chieffi P, Fusco A, Portella G. Aurora B overexpression associates with the thyroid carcinoma undifferentiated phenotype and is required for thyroid carcinoma cell proliferation. J. Clin. Endocrinol. Metab. 2005; 90:928–935. [PubMed: 15562011]

25. Schweppe RE, Klopper JP, Korch C, Pugazhenthi U, Benezra M, Knauf JA, Fagin JA, Marlow LA, Copland JA, Smallridge RC, Haugen BR. Deoxyribonucleic acid profiling analysis of 40

human thyroid cancer cell lines reveals cross-contamination resulting in cell line redundancy and misidentification. J. Clin. Endocrinol. Metab. 2008; 93:4331–4341. [PubMed: 18713817]

26. Wiseman SM, Masoudi H, Niblock P, Turbin D, Rajput A, Hay J, Bugis S, Filipenko D, Huntsman D, Gilks B. Anaplastic thyroid carcinoma: Expression profile of targets for therapy offers new insights for disease treatment. Ann. Surg. Oncol. 2007; 14:719–729. [PubMed: 17115102]

27. Gizatullin F, Yao Y, Kung V, Harding MW, Loda M, Shapiro GI. The Aurora kinase inhibitor VX-680 induces endoreduplication and apoptosis preferentially in cells with compromised p53-dependent postmitotic checkpoint function. Cancer Res. 2006; 66:7668–7677. [PubMed: 16885368]
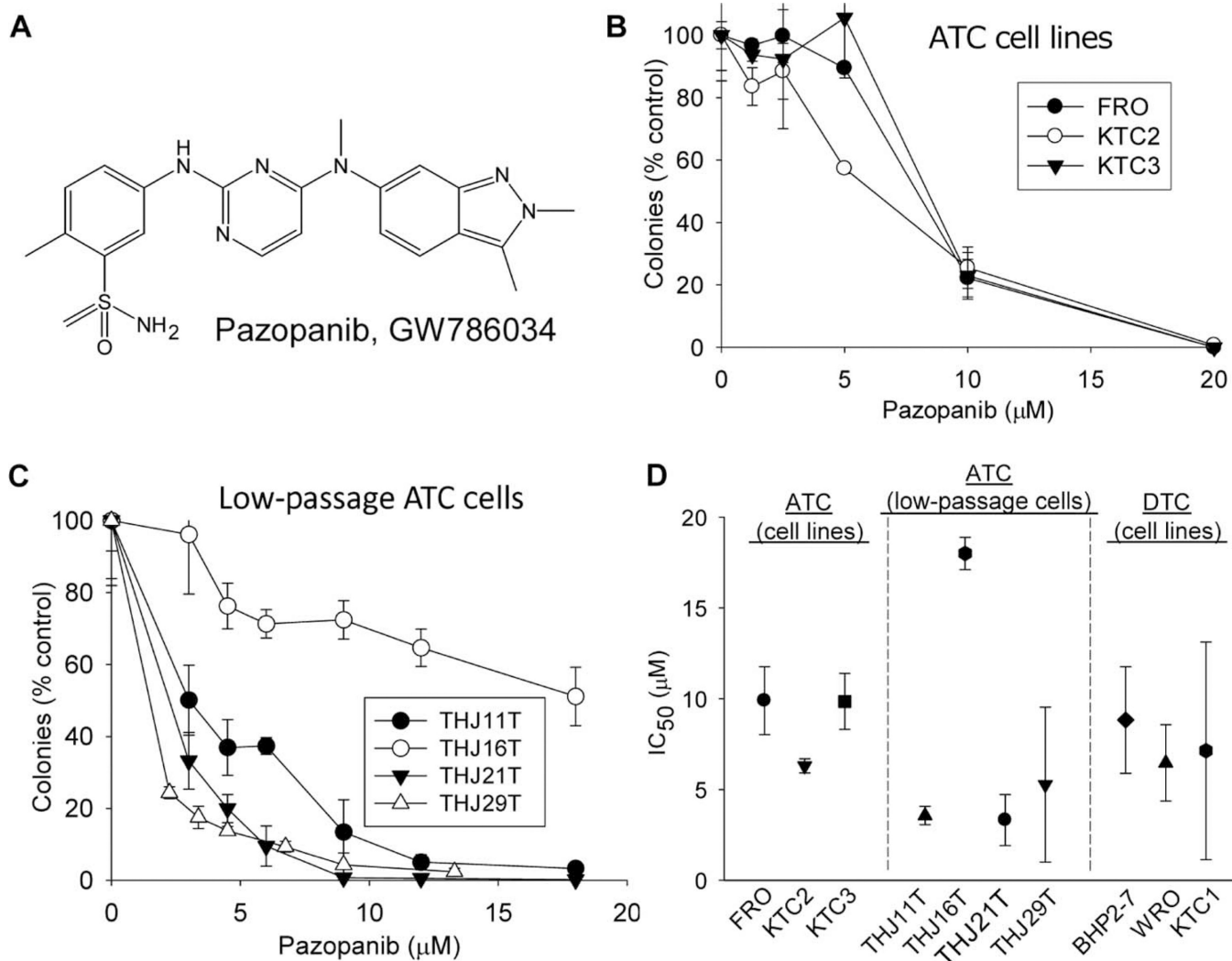
Fig. 1.
Pazopanib has single-agent in vitro antineoplastic activity in ATC. (**A**) Chemical structure of pazopanib. (**B** and **C**) Growth-inhibitory effects of pazopanib (continuous drug exposures) in three ATC cell lines (B) and in four patient primary low-passage ATC cell culture models (C). In (B) and (C), results of representative colony-forming assays are shown (each data point indicates the mean of triplicate results; error bars indicate 1 sample SD). (**D**) Summary data indicating IC_{50} mean and SD values for each cell line/culture compared to three DTC cell lines [all results reflect more than three replicate experiments as shown in (B) and (C)].
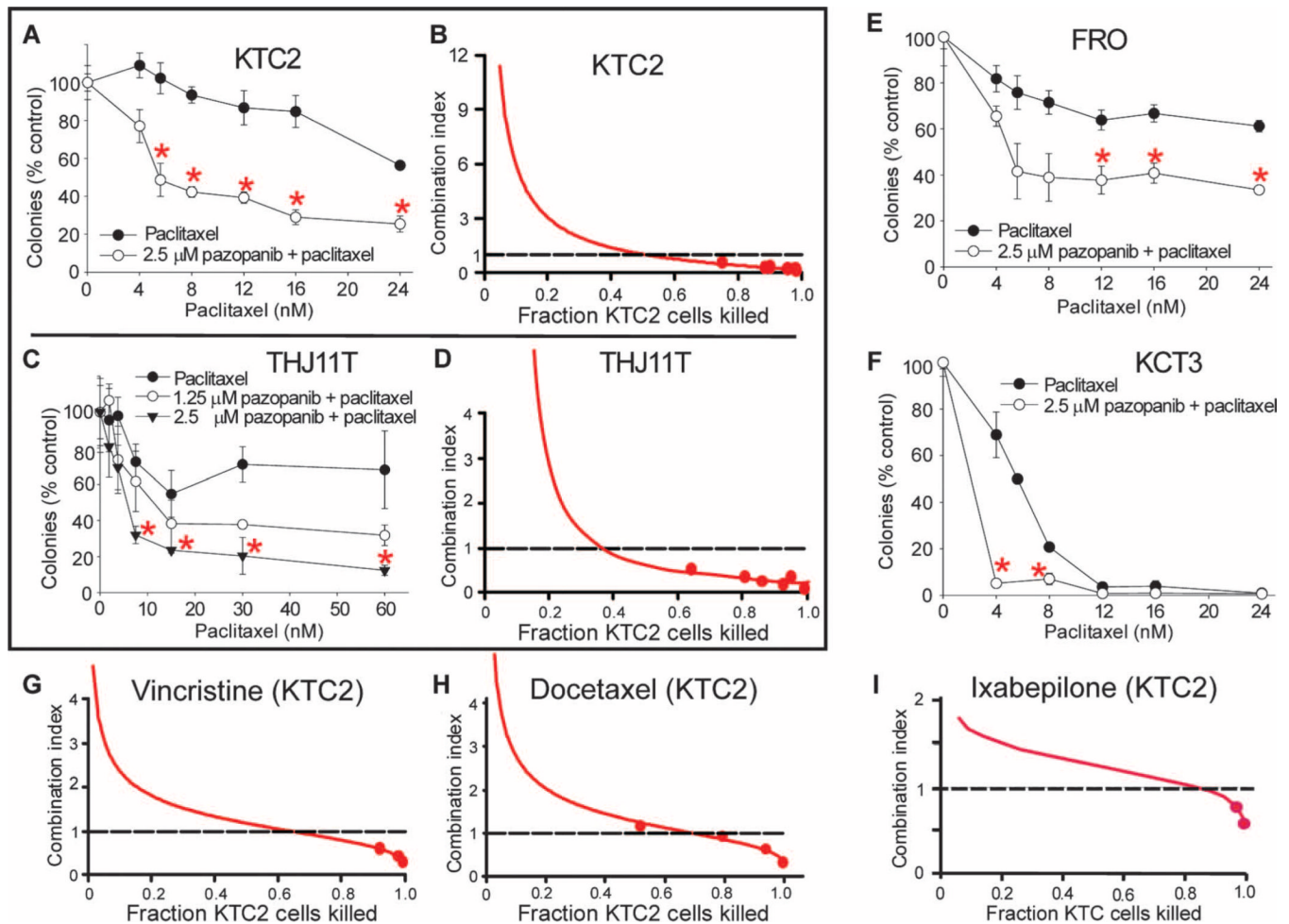
Fig. 2.
Pazopanib enhances the effects of paclitaxel (as well as of other antimicrotubule inhibitors including vincristine, docetaxel, and ixabepilone) in ATC in vitro model systems. (**A** to **F**) Pazopanib potentiates the antineoplastic effects of paclitaxel in KTC2 (A and B), THJ11T (C and D), FRO (E), and KTC3 (F) ATC cells. (A), (C), (E), and (F) show results of representative colony-forming assays (each data point indicates the mean ± SD of triplicate results, with each experiment replicated more than three times); dose-responsive synergistic effect is also shown in (C). (B and D) Results assessing pazopanib/paclitaxel synergy using a distinct approach, median-effect analyses, in KTC2 and THJ11T models, respectively. (**G** to **I**) Analogous results for KTC2 ATC cells treated alternatively with pazopanib + vincristine, pazopanib + docetaxel, or pazopanib + ixabepilone, respectively. In CI plots [per the method of Chou and Talalay (14)], CI < 1 indicates synergy, CI = 1 indicates additivity, and CI > 1 indicates antagonism. Error bars indicate 1 sample SD; red asterisks indicate differences between paclitaxel and pazopanib/paclitaxel (*P* < 0.01); all CI plots are representative of three or more distinct experiments, with all data points in all experiments done in triplicate.
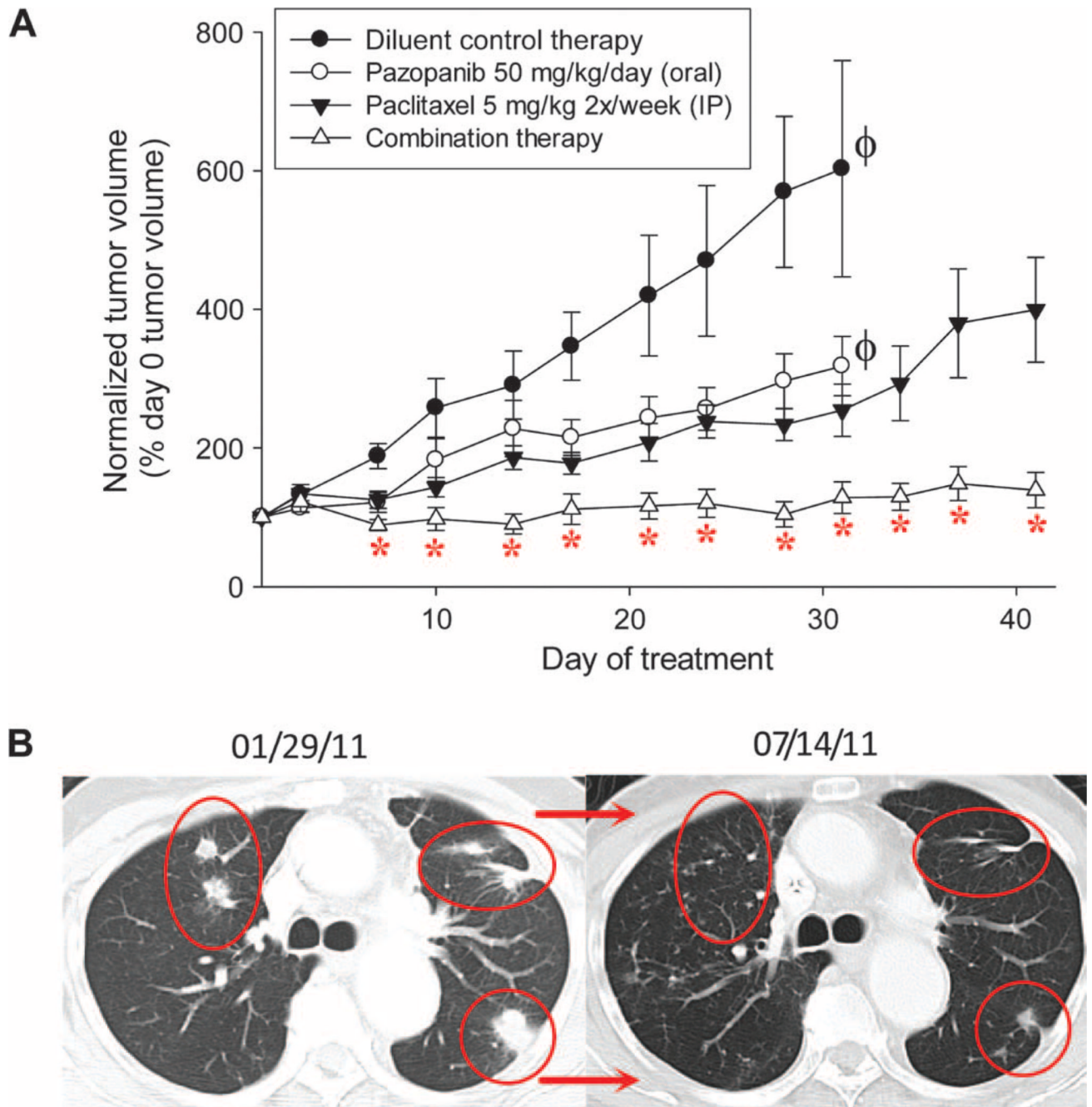
Fig. 3.
Pazopanib and paclitaxel combine to yield enhanced cytotoxic effects in vivo and a durable clinical response in a patient. (**A**) In vivo anti-tumor effects of single-agent or combined pazopanib and paclitaxel KTC2 ATC xenograft model. Error bars indicate 1 sample SD; *P < 0.001 for differences between combination therapy effects relative to the respective single-agent effects at various time points (differences between diluent- and paclitaxel- or pazopanib-treated animals also achieved statistical significance in each instance); 10 animals per treatment group. Absent tumor measurements at later time points in diluent and pazopanib treatment arms (indicated by φ) reflect the need to euthanize animals because of

excessive tumor burden. IP, intraperitoneally. (**B**) Effects of combined pazopanib (800 mg/ day, orally) and paclitaxel (80 mg/m^2 per week, intravenously) therapy in a pilot ATC patient; representative computed tomography images depicting effects on lung metastases are shown before therapy and after ~6 months of therapy.
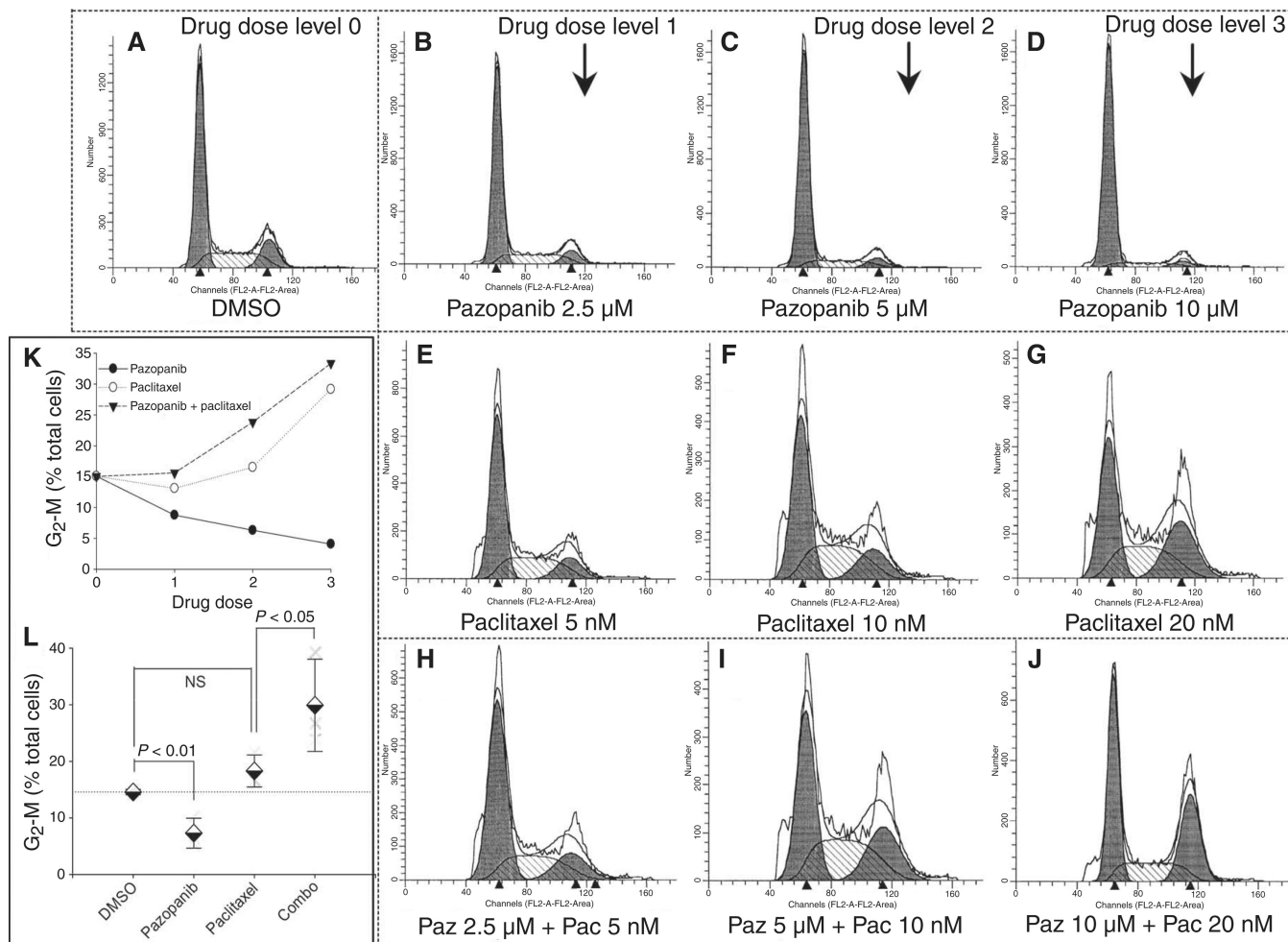
Fig. 4.
Pazopanib alters the effects of paclitaxel on cell cycle distribution in KTC2 ATC cells. (**A** to **D**) Effects of pazopanib alone. (**E** to **G**) Effects of paclitaxel alone. (**H** to **J**) Combined effects of paclitaxel and pazopanib. (**K** and **L**) Summary data related to effects on G_2-M phase of the cell cycle are shown in (K) for this experiment, with results across three replicate analogous experiments (dose level 2) summarized in (L). All depicted experiments were gaited to specifically exclude subdiploid debris. DMSO, dimethyl sulfoxide.
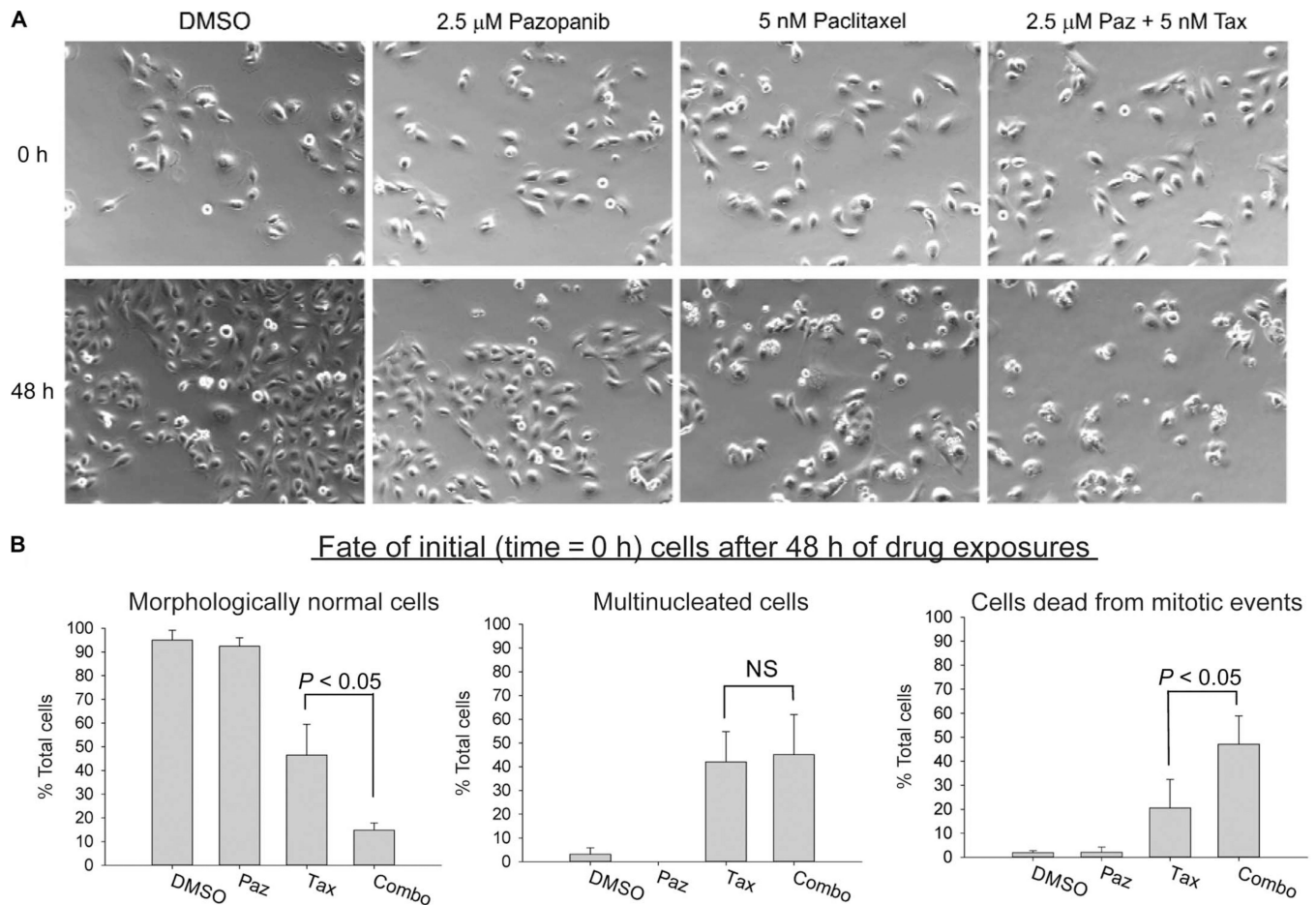
Fig. 5.
Pazopanib and paclitaxel combine to affect cell fate in KTC2 ATC cells. (**A**) Images (captured from real-time video microscopy) showing morphological effects of single-agent and combined pazopanib (Paz) and paclitaxel (Tax) relative to diluent control. (**B**) Summary data indicating effects of single-agent and combined pazopanib and paclitaxel relative to diluent control on KTC2 cell fate after 48-hour exposures across three replicate experiments. Left panel, morphologically normal cells; middle panel, multinucleated cells; right panel, cells dying after dysfunctional mitosis [all expressed as % total time = 0 cells; data shown in (A) are representative of three independent experiments]. Error bars in (B) represent 1 sample SD, triplicate experiments; NS, not statistically significant; significance levels shown for one-sided *t* tests.
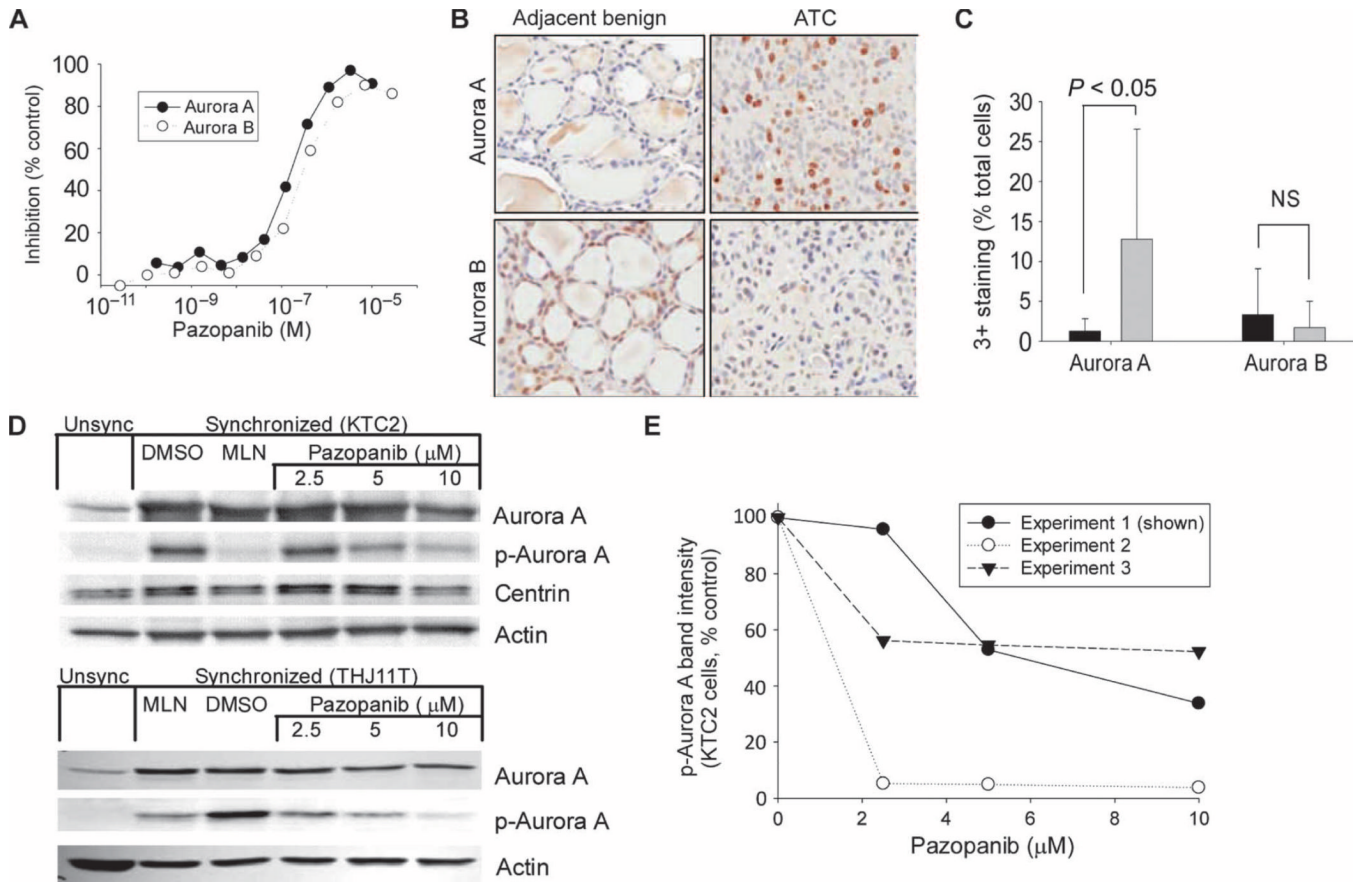
Fig. 6.
Pazopanib alters aurora A or B kinase activity in cell-free assays and aurora A phosphorylation in intact KTC2 or THJ11T ATC cells; aurora A levels are higher in patient ATC tumors in comparison to normal thyroid tissue. (**A**) Results of cell-free aurora A or B kinase activity assays as a function of pazopanib concentration. (**B** and **C**) Representative results of immunohistochemical staining for aurora A and B in patient ATC samples relative to nonneoplastic control thyroid tissue (B), with tabulated patient data shown in (C), indicating aurora A, but not aurora B, overexpression in primary human ATC specimens (black bars, nonneoplastic; gray bars, ATC; error bars represent 1 sample SD; NS, not statistically significant, significance levels shown for two-sided t test). (**D**) Effects of pazopanib on total and phospho–aurora A as a function of pazopanib concentration in synchronized mitotic KTC2 or THJ11T primary ATC cells, respectively; results for unsynchronized cells are shown on the left as controls, with the effects of diluent (DMSO) or the specific aurora kinase A inhibitor MLN8237 (25 nM) on synchronized/mitotic cells also shown as negative and positive controls, respectively. Results are representative of three independent experiments. (**E**) Summary results of three independent KTC2 experiments including that shown in (D), indicating effects of varying pazopanib concentrations on phospho–aurora A immunoblotting across replicate experiments.
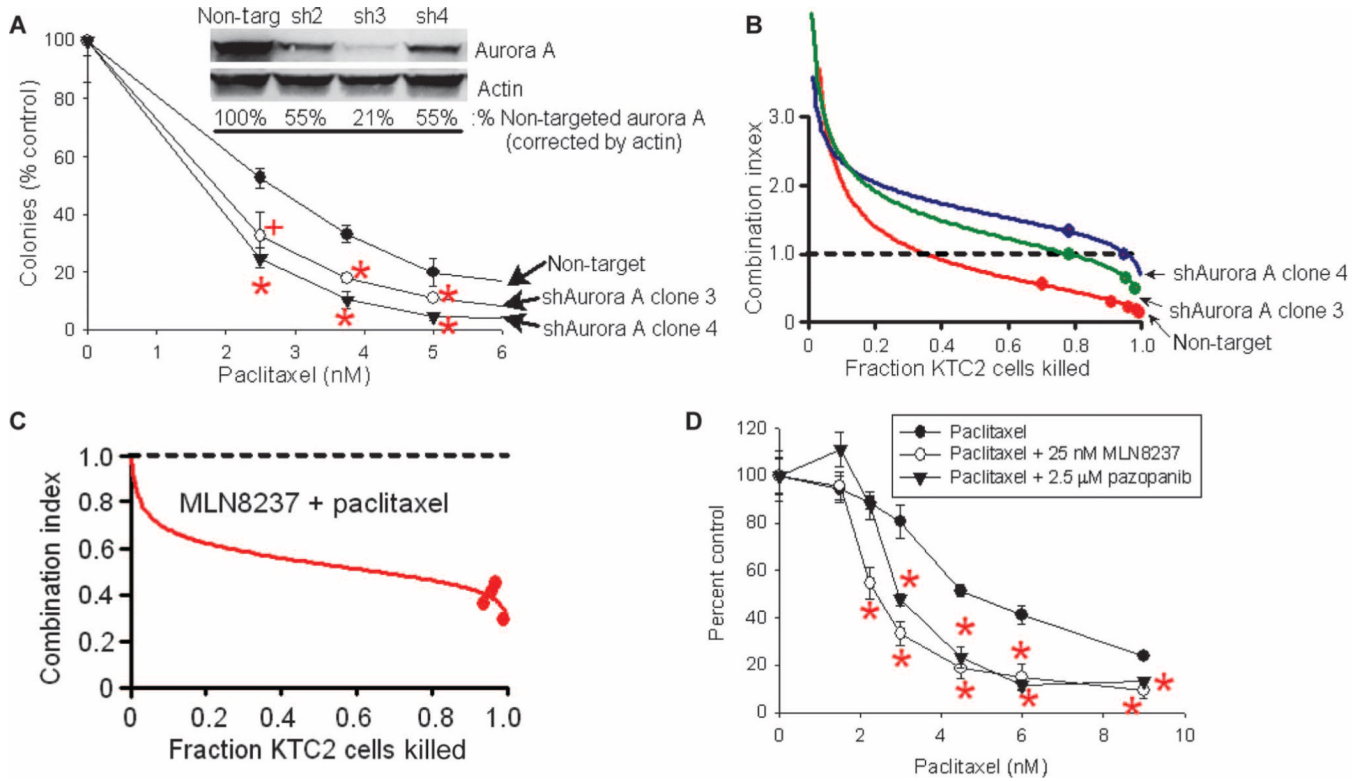
Fig. 7.
Aurora A shRNA knockdown and treatment with the specific aurora A inhibitor MLN8237 similarly alter the effects of paclitaxel monotherapy as well as the combined effects of paclitaxel and pazopanib. (**A**) Impact of aurora A shRNA knockdown on the effects of paclitaxel alone (KTC2 cells). Inset, results of immunoblotting for aurora A compared to actin loading control in parental/(nontargeted) cells compared to three shRNA aurora A knockdown clones (sh2 to sh4). (**B**) Effects of aurora A shRNA knockdown on combined paclitaxel/pazopanib synergy. (**C**) Aurora A inhibition by MLN8237 results in synergy with paclitaxel in KTC2 ATC cells as assessed by median-effect analysis. (**D**) Impact of aurora A inhibition by MLN8237 (25 nM) compared to that of pazopanib (2.5 μM) on the effects of paclitaxel in KTC2 ATC cells. In (B) and (C), median-effect analysis results per Chou and Talalay (13) are shown: CI values of 1, <1, or >1 indicate additivity, synergy, or antagonism, respectively. In (A) and (D), error bars indicate 1 sample SD; $^{+}P < 0.05$, $^{*}P < 0.01$ relative to controls. All panels show representative results of more than three replicate assays.